

Received January 9, 2019, accepted February 5, 2019, date of publication February 26, 2019, date of current version March 26, 2019.

Digital Object Identifier 10.1109/ACCESS.2019.2900499

Fault Monitoring Based on Adaptive Partition Non-Negative Matrix Factorization for Non-Gaussian Processes

YAN WANG¹, SHI-MENG YUAN¹, DAN LING¹, YU-BO ZHAO¹,
XIAO-GUANG GU^{2,3}, AND BO-YI LI¹

¹School of Electrical and Information Engineering, Zhengzhou University of Light Industry, Zhengzhou 450002, China

²Intelligent Manufacturing Big Data Platform (Zhengzhou) R&D Center, Zhengzhou Normal University, Zhengzhou 450044, China

³School of Business, Nanjing University, Nanjing 210093, China

Corresponding author: Xiao-Guang Gu (guxiaoguang86@126.com)

This work was supported in part by the National Nature Science Foundation of China under Grant 61603346 and Grant 61603347, in part by the key research projects of Henan Higher Education Institutions under Grant 19A413003, in part by the Doctor Startup Foundation of the Zhengzhou University of Light Industry under Grant 2015BSJJ024 and Grant 13501050058, and in part by the Open Research Fund of Zhengzhou Normal University.

ABSTRACT In this paper, a new fault monitoring method based on adaptive partitioning non-negative matrix factorization (APNMF) is presented for non-Gaussian processes. Non-negative matrix factorization (NMF) is a new dimension reduction technique, which can effectively deal with Gaussian and non-Gaussian data. However, the NMF model of traditional fault monitoring method is time-invariant and cannot provide fault warning for the slowly changing industrial process. Therefore, this paper proposes an adaptive partition NMF algorithm with non-fixed sub-block NMF models. First, the process variables under different operating conditions of the system are divided into several sub-variable spaces adaptively by the complete linkage algorithm. Then, the global variables space and each sub-variable space are modeled by the NMF method. Finally, the kernel density estimation (KDE) method is adapted to calculate the control limits of the defined statistical metrics. The proposed method makes full use of intra-block local information and inter-block global information, which improves diagnostic performance. The experimental results of a numerical process and the Tennessee Eastman (TE) benchmark process show that the proposed method improves the accuracy of fault monitoring compared with the existing algorithms.

INDEX TERMS Fault monitoring, adaptive partitioning, non-negative matrix factorization, non-Gaussian processes, kernel density estimation.

I. INTRODUCTION

With modern industrial processes become more and more complex, many industrial processes such as chemical processes usually consist of mass data that are random, non-linear, uncertain, and dynamic. The increasing demands for safe operation of industrial plants continue to gain attention of research in process monitoring. Multivariate statistical process monitoring (MSPM) is a powerful data-driven technology to detect and identify changes and faults [1]. The nature of MSPM is to transform high-dimensional data into lower-dimensional data and obtain important information in low-dimensional data, especially in large systems.

The associate editor coordinating the review of this manuscript and approving it for publication was Mark Kok Yew Ng.

Typical MSPM techniques include principal component analysis (PCA), partial least squares (PLS), canonical variable analysis (CVA), independent component analysis (ICA) and so on [2]–[5].

PCA is a widely used reduction technique that is implemented by projecting variables onto a smaller new set of uncorrelated variables. For the past years, several PCA based methods had been successfully applied to online monitoring of industrial processes, especially chemical processes [6]. In fact, PCA gradually presents some limitations in fault monitoring and isolation. One of the drawbacks of the PCA based fault diagnosis method is that the PCA model constructed by the global data ignores the local information of process data. However, the local information can monitor the local changes caused by fault and improve the performance of

fault diagnosis. To solve these problems, it is common to divide the process variables into blocks, diagnose each block separately, and then further determine which sub-block failed. Lee and Vanrolleghem [7] proposed a new monitoring method for batch process based on adaptive multi-block MPCA algorithm. Liu *et al.* [8] proposed an adaptive partitioning principal component analysis (APPCA) method for fault diagnosis using local information within the block and the global information between the blocks. The above methods analyzed both global and local models, which greatly improved the efficiency of fault diagnosis.

Another limitation of PCA is that the process measurements being monitored must follow a Gaussian distribution. In actual industrial production, most process measurements not only contain Gaussian distribution, but also may contain non-Gaussian distribution owing to the frequent occurrence of special cause events. If the traditional PCA method is used for fault monitoring at this time, the statistical characteristics of the process will be weakened, resulting in inaccurate process performance analysis and a large number of process failures. In order to solve the non-Gaussian problem, some relevant scholars proposed ICA algorithm [9], [10]. Different from the principal elements obtained by the PCA algorithm, the latent variables extracted by ICA, which are called the independent components (ICs), are assumed to be non-Gaussian and mutually independent. In fact, the ICA algorithm not only removes the correlation between variables, but also contains high-order statistics. Therefore, ICA can contain more useful information than PCA. In recent years, non-negative matrix (NMF), multi-label learning (MLL), semisupervised learning (SSL) have been widely used in feature extraction of images [11]–[13].

The non-negative matrix (NMF) is a new dimension reduction method proposed by Lee and Seung [14], [15]. Compared with the traditional MSPC monitoring methods, the NMF algorithm has no other limitations on the measurement data except for non-negative [16]. Measurement data in industrial processes may not meet non-negative conditions, such as temperature, pressure and other sensor readings may be negative. However, the measurements of these sensors can be adjusted so that they are not negative. Therefore, in general, industrial process data can basically meet the requirements of NMF. Therefore, NMF has a wider range of applications. In addition, the NMF algorithm can capture the local characteristics of the data from a large amount of data, and has better explanatory ability than the traditional MSPC methods.

In recent years, the NMF method has attracted more and more attention and shown the superiority in many successful applications, e.g., data mining, pattern recognition and clustering [11], [17], [18]. However, the application of NMF method in fault monitoring is relatively rare. Li *et al.* [19] proposed a fault diagnosis method for non-Gaussian process based on the NMF algorithm. Later, they proposed a generalized non-negative matrix projection (GNMP) based on the projection non-negative matrix

factorization (PNMF) [20]. This method had no non-negative constraint on the original data, which greatly expanded the application range of NMF algorithm. Chen *et al.* [21] proposed a new method to separate the feature automatically using the supervised NMF. Zhu *et al.* [22] clustered the multi-mode process data by a traditional NMF and proposed a novel multi-mode process monitoring approach. However, the NMF model in the above fault monitoring methods is time-invariant. Since many industrial processes often change slowly, the application of fixed model based fault detection may reduce the accuracy of fault monitoring.

In order to improve the accuracy of fault monitoring, the paper proposes a fault monitoring method based on adaptive partition non-negative matrix factorization (APNMF). The main contributions of this paper are as follows. (1) The proposed method is purely data-driven and can be used for fault monitoring of non-Gaussian processes. This is especially important when process knowledge is scarce. (2) Fault diagnosis models can be dynamically updated. Different operating conditions have different block results, which makes the fault detection results more interpretable. (3) The sub-block model can not only reflect the local behavior of process change, but also improve the accuracy of fault detection by combining local fault detection results. Compared with existing algorithms, the proposed method can obtain higher fault detection rate and lower delay time. The effectiveness of this method is demonstrated by simulation results of a numerical process and the TE process.

The rest of the paper is organized as follows: Section 2 introduces the related algorithms including PCA, NMF and KDE. Section 3 presents the APNMF algorithm. Section 4 describes the monitoring steps of fault monitoring method based on the APNMF algorithm. In Section 5, the experiment results of a numerical process and the TE process verify the effectiveness of the proposed algorithm. Finally, the conclusions and future work are discussed in Section 6.

II. RELATED MSPM TECHNIQUES

A. PRINCIPAL COMPONENT ANALYSIS (PCA)

PCA is a typical data statistical analysis method, which is widely used in process control, fault diagnosis and other fields [2]. Consider a measurement matrix $X^T = [x_1, x_2, \dots, x_M]^T \in R^{M \times d}$, for d process variables with M measurements for each variable. Before establishing the PCA model, it is needed to preprocess X^T . Then the covariance matrix is calculated and the eigenvalues are decomposed. According to the descending order of eigenvalues, the number of principal elements k ($k \leq d$) is selected by contribution method. Thus, X^T can be decomposed by PCA as:

$$X^T = \hat{X}^T + E_{PCA} = TP^T + E_{PCA}, \quad T = X^T P \quad (1)$$

where $T \in R^{M \times k}$ is the score matrix and $P \in R^{d \times k}$ is the load matrix. \hat{X}^T and $E_{PCA} \in R^{M \times d}$ are the principal component subspace (PCS) and residual subspace (RS) of the measurement matrix X^T respectively.

In case of fault monitoring, the monitoring indicators of PCS and RS are Hotelling's T^2 and SPE respectively, both of which can be calculated as follows:

$$T^2 = x^T P \Lambda^{-1} P^T x \quad (2)$$

$$SPE = x^T (I - PP^T)x \quad (3)$$

where Λ is the diagonal matrix associated with the PCS.

B. NON-NEGATIVE MATRIX FACTORIZATION(NMF)

The NMF algorithm was firstly proposed by Lee and Seung [14]. Given a non-negative data matrix $X = [x_1, x_2, \dots, x_M] \in R^{d \times M}$, the main idea of the NMF algorithm is to approximate X as the product of two non-negative matrices $W \in R^{d \times k}$ and $H = [h_1, h_2, \dots, h_M] \in R^{k \times M}$, which is of the form:

$$X \approx WH \quad (4)$$

where W is the base matrix, and H is the coefficient matrix. The selection of lower dimensional order k satisfies $(d + M)k \leq dM$.

The standard NMF algorithm can be reduced to a nonlinear optimization problem with an objective function measuring the quality of the low rank approximation. Lee and Seung [15] defined two objective functions and formulated the iteration rules of W and H , as shown in equations (5) and (6):

$$F_1 = \|X - WH\|^2 \quad (5)$$

s.t. $X \geq 0, W \geq 0, H \geq 0$

$$F_2 = \sum_{i,j} \left(X_{ij} \lg \frac{X_{ij}}{(WH)_{ij}} - X_{ij} + (WH)_{ij} \right) \quad (6)$$

s.t. $X \geq 0, W \geq 0, H \geq 0$

The objective function (5) is relatively simple to implement and has been effectively applied in many literature, such as [16], [19], and [20]. Hence, the paper uses the target function shown in equation (5).

The local optimal iteration method for the objective function (5) is shown as:

$$W_{ia} \leftarrow W_{ia} \frac{(XH^T)_{ia}}{(WHH^T)_{ia}} \quad (7)$$

$$H_{ia} \leftarrow H_{ia} \frac{(W^T X)_{aj}}{(W^T WH)_{aj}} \quad (8)$$

The objective function F_1 is invariant under these updates if and only if W and H are at a stationary point. The base matrix W retains the structure and space relation of the matrix X , and the coefficient matrix H expresses the low order approximate matrix of the matrix X . Therefore, the fault monitoring model of NMF algorithm is shown as:

$$X = W\hat{H} + E \quad (9)$$

where $\hat{H} = (W^T W)^{-1} W^T X$ is the low order approximate matrix and E is residual matrix.

To reflect the process status for industrial process data, N^2 and SPE are proposed as process monitoring indices, which are [19]:

$$N^2 = \hat{h}_j^T \hat{h}_j, \quad j = 1, 2, \dots, M \quad (10)$$

$$SPE = (x_j - \hat{x}_j)^T (x_j - \hat{x}_j) \quad (11)$$

where $\hat{h}_j \in R^k$ and $x_j \in R^d$ are the j th column vectors of the matrix \hat{H} and X , respectively. In addition, \hat{x}_j can be obtained by $\hat{x}_j = W\hat{h}_j$.

C. KERNEL DENSITY ESTIMATION (KDE)

In PCA monitoring, the control limits are based on a specified distribution by assuming that potential variables follow Gaussian distribution. However, for the non-Gaussian process discussed in this paper, the control limits of N^2 and SPE cannot be calculated directly from a particular approximate distribution. In this paper, the KDE method is applied to estimate the probability density function (PDF) of N^2 and SPE , and then calculate the corresponding control limit [23].

Let $Q = \{q_i, i = 1, 2, \dots, n\}$ represent a samples set and its PDF can be calculated as follows:

$$\hat{p}(q) = \frac{1}{n\omega} \sum_{i=1}^n K\left(\frac{q - q_i}{\omega}\right) \quad (12)$$

where q_i is the value of the i th sample, n is the number of the observed samples, ω is the bandwidth or smooth parameter, and $K(\cdot)$ is a kernel function that satisfies the following conditions:

$$\int_{-\infty}^{\infty} K(q) dq = 1, \quad K(q) \geq 0 \quad (13)$$

In fact, the selection of kernel function has little effect on the accuracy of the KDE, which has been indicated in [19] and [20]. Usually, Gaussian kernel is a popular choice. However, the selection of the bandwidth ω has a great influence on the accuracy of the results. If ω is too small, the density estimator will be under-smoothed, while if ω is too large, the density estimator will be over-smoothed. Therefore, the optimal value of bandwidth needs to be found as much as possible. By using the least square cross-validation and the contrast methods, Mugdadi and Ahmad [24] deduced that the bandwidth was:

$$\omega = 1.06\sigma n^{-0.2} \quad (14)$$

where σ is the standard deviation.

After the PDF is calculated, the cumulative density function (CDF) can be expressed as:

$$\hat{P}(q < \theta) = \int_{-\infty}^{\theta} \hat{p}(q) dq \quad (15)$$

Afterwards, the confidence degree is given by 99%. The corresponding confidence region can be obtained based on the CDF and confidence degree.

III. ADAPTIVE PARTITION NON-NEGATIVE MATRIX FACTORIZATION (APNMF)

APNMF is a method of data partitioning using residual matrix. It can not only update the fault diagnosis model dynamically, but also deal with non-Gaussian data effectively.

All of the NMF based algorithms are sensitive to the initialization of two non-negative matrices W and H . A good initialization value will facilitate the fast convergence of NMF and obtain a better local optimal solution. There exist different NMF initialization schemes based on random values or singular value decomposition (SVD) [19], [20], [22]. It is noted that the measurement matrix X^T can be decomposed by PCA as $X^T = TP^T + E$. In this paper, the absolute value of load matrix P and the transpose of score matrix T are used to initialize the basis matrix W and the coefficient matrix H . This initialization approach is very simple and could make NMF get a steady result and even faster. In order to show the effectiveness of the proposed initialization method, the following error function is defined:

$$error = \frac{\|X - WH\|^2}{\|X\|^2} \quad (16)$$

Consider two data matrices $X_n \in R^{d \times M_n}$ and $X_f \in R^{d \times M_f}$. X_n is the normal data matrix and X_f is the fault data matrix collected from one fault case. M_n and M_f are the number of sample. The fault monitoring model of NMF algorithm is as follows:

$$\begin{aligned} X_n &= W_n \hat{H}_n + E_n \\ \hat{H}_n &= (W_n^T W_n)^{-1} W_n^T X_n \end{aligned} \quad (17)$$

with \hat{H}_n is the low order approximate matrix and E_n is residual matrix.

For the faulty data matrix X_f , residuals E_f can be obtained as:

$$E_f = X_f - W_n (W_n^T W_n)^{-1} W_n^T X_f \quad (18)$$

The residual subspace can usually describe the material energy balance [8]. Since the failure can cause material energy imbalance and change the correlation between variables, the residual are very sensitive to process failures. Therefore, the changes in the correlation between process variables can be described according to the residual matrix in the fault state [8]. The variable partitioning method is performed based on the NMF residuals of a fault state.

Assume matrix $R_f \in R^{d \times d}$ denote the correlation between process variables in the fault state. $R_{f,ij}$ represents the degree of correlation between the variable i and j . Pearson's correlation coefficients was selected to measure the degree of correlation between variables, which is

$$R_{f,ij} = \frac{E[(E_{f,i} - \bar{E}_{f,i})(E_{f,j} - \bar{E}_{f,j})]}{\sqrt{\sum_{i=1}^{N_f} (E_{f,i} - \bar{E}_{f,i})^2} \sqrt{\sum_{j=1}^{N_f} (E_{f,j} - \bar{E}_{f,j})^2}} \quad (19)$$

TABLE 1. A framework of APNMF algorithm.

| Proposed APNMF algorithm | |
|--------------------------|--|
| 1. | Get $X_n \in R^{d \times M_n}$. Decompose the data set X_n^T by PCA, choose the first k PCs, and obtain the loading matrix $P \in R^{d \times k}$ and the score matrix $T \in R^{k \times M_n}$. |
| 2. | Initialize $W_n = \{[p_{ij}], p_{ij} \in P\}$ and $H_n = \{[t_{ij}], t_{ij} \in T\}$. |
| 3. | Repeat running the following for a certain times until the Euclidean distance $F_1 = \ X_n - W_n H_n\ ^2$ is invariant. |
| | $W_{ia} \leftarrow W_{ia} \frac{(X_n H_n^T)_{ia}}{(W_n H_n H_n^T)_{ia}},$ $H_{ia} \leftarrow H_{ia} \frac{(W_n^T X_n)_{aj}}{(W_n^T W_n H_n)_{aj}}.$ |
| 4. | Obtain the base matrix $W_n \in R^{d \times k}$ and coefficient matrix $H_n \in R^{k \times M_n}$. |
| 5. | Get $X_f \in R^{d \times M_f}$ and calculate the residual matrix $E_f = X_f - W_n (W_n^T W_n)^{-1} W_n^T X_f$. |
| 6. | Calculate Pearson's correlation coefficients R_f , |
| | $R_{f,ij} = \frac{E[(E_{f,i} - \bar{E}_{f,i})(E_{f,j} - \bar{E}_{f,j})]}{\sqrt{\sum_{i=1}^{N_f} (E_{f,i} - \bar{E}_{f,i})^2} \sqrt{\sum_{j=1}^{N_f} (E_{f,j} - \bar{E}_{f,j})^2}}.$ |
| 7. | Obtain significant horizontal matrix S_f by t-test of R_f . |
| 8. | Output the result sub-blocks $C_i (i = 1, 2, \dots, b)$ by the linkage(S_f , 'complete'). |

with $E_{f,i}$ and $E_{f,j}$ are the residuals of the i th and j th variables respectively, and $\bar{E}_{f,i}$ and $\bar{E}_{f,j}$ are the average of $E_{f,i}$ and $E_{f,j}$ respectively.

Obtain significant horizontal matrix S_f by t-test of R_f . Each $S_{f,ij}$ in the matrix S_f represents the degree of correlation between the variable i and the variable j , ranging from 0 to 1. The smaller the value of $S_{f,ij}$, the stronger correlation between the two variables. Define the matrix S_f as distance matrix and partition the variables into some sub-blocks $C_i (i = 1, 2, \dots, b)$ by the complete linkage algorithm [25]. In summary, the APNMF algorithm proposed in this section is shown in Table 1.

With the above APNMF method, each sub-block data $X_i \in R^{d_i \times M} (i = 1, 2, \dots, b)$ with $d_1 + d_2 + \dots + d_b = d$ is constructed by the variable of sub-blocks C_i . Let W_g, H_g, E_g, W_i, H_i and E_i represent the basis matrix, coefficient matrix and residual matrix of the global model and i th sub-block model respectively. The global and local monitoring models of NMF can be constructed as follows:

$$\begin{aligned} X_g &= W_g \hat{H}_g + E_g \\ X_i &= W_i \hat{H}_i + E_i, \quad i = 1, 2, \dots, b \end{aligned} \quad (20)$$

with $\hat{H}_g = (W_g^T W_g)^{-1} W_g^T X_g$ and $\hat{H}_i = (W_i^T W_i)^{-1} W_i^T X_i$.

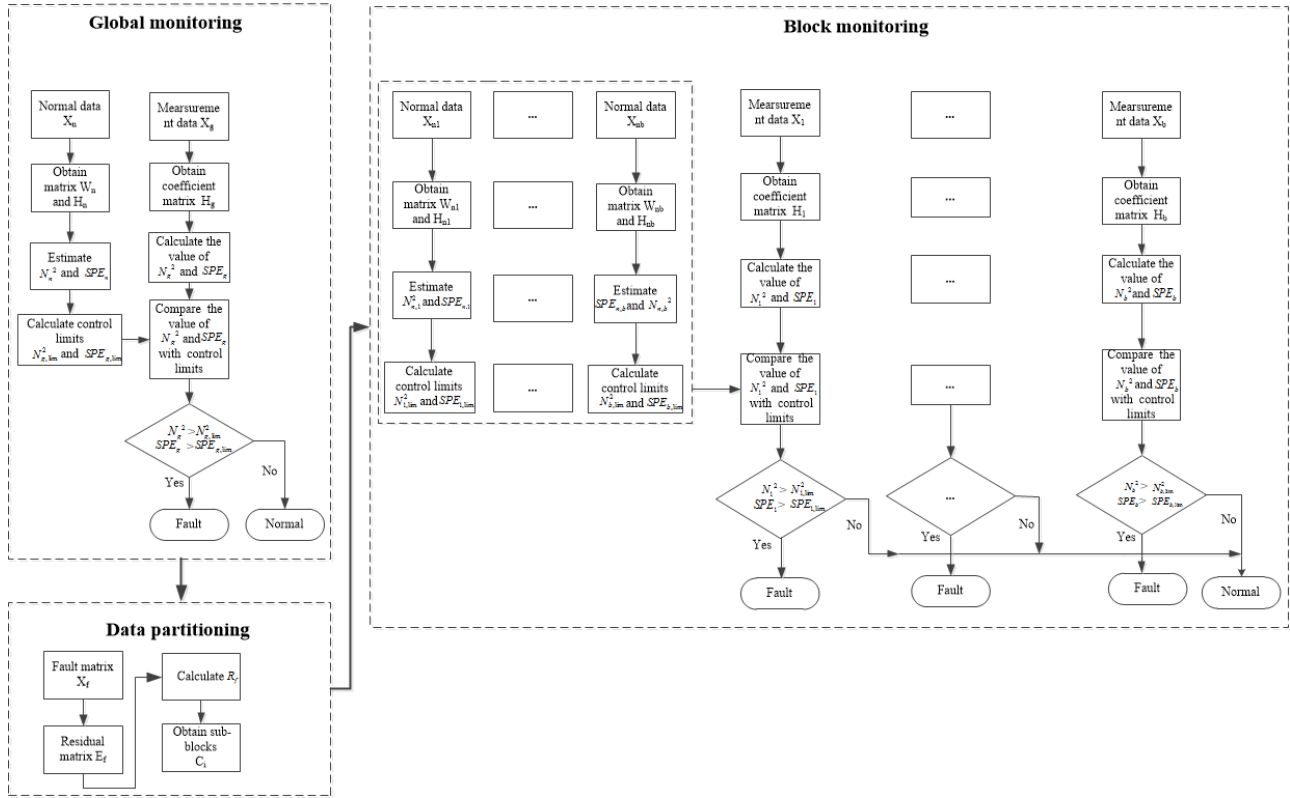


FIGURE 1. Schematic diagram of the APNMF monitoring method.

IV. NON-GAUSSIAN PROCESS MONITORING BASED ON APNMP

The proposed fault monitoring method mainly includes three stages: global fault monitoring, data adaptive partitioning and block fault monitoring. The schematic diagram of the proposed APNMF monitoring method is shown in Figure 1, and the detailed steps are presented as follows:

A. GLOBAL FAULT MONITORING

- (1) Collect the normal history data matrix $X_n \in R^{d \times M_n}$ with non-negative elements. The initial value of NMF algorithm is obtained by PCA and the base matrix W_n and coefficient matrix H_n are calculated using (7) and (8) respectively.
- (2) Construct the monitoring statistic N_n^2 and SPE_n of by (10) and (11). The control limits $N_{g,lim}^2$ and $SPE_{g,lim}$ of monitoring statistics are calculated by KDE algorithm.
- (3) Collect the global measurement data $X_g \in R^{d \times M}$ with non-negative elements. The coefficient matrix $H_g = W_n^T X_g$ is obtained.
- (4) Construct the monitoring statistic N_g^2 and SPE_g using (10) and (11), which are compared with the control limits $N_{g,lim}^2$ and $SPE_{g,lim}$. If one of N_g^2 and SPE_g statistics exceeds the corresponding control limit, the process fault will be detected.

B. DATA PARTITIONING

- (1) Construct the residual matrix E_f of fault data $X_f \in R^{d \times M_f}$ which are detected by the global fault monitoring.
- (2) Calculate the Pearson's correlation coefficients R_f using (19) and obtain the significant horizontal matrix S_f by t-test of R_f .
- (3) Partition the variables into different sub-blocks $C_i (i = 1, 2, \dots, b)$ using the complete linkage algorithm.

C. BLOCK FAULT MONITORING

- (1) Construct the sub-block normal data matrix $X_{n,i} \in R^{d_i \times M_n} (i = 1, 2, \dots, b)$ according to sub-block $C_i (i = 1, 2, \dots, b)$ and obtain the base matrix $W_{n,i}$ and coefficient matrix $H_{n,i}$ of each sub-block $X_{n,i}$ using (7) and (8).
- (2) Construct the monitoring statistic $N_{n,i}^2$ and $SPE_{n,i}$ of each sub-block by (10) and (11). Calculate the control limits $N_{i,lim}^2$ and $SPE_{i,lim}$ of monitoring statistics by KDE algorithm.
- (3) Construct the sub-block measurement data matrix $X_i \in R^{d_i \times M} (i = 1, 2, \dots, b)$ and calculate the monitoring statistic N_i^2 and SPE_i of each sub-block X_i .
- (4) Calculate $b + 1$ pairs of N^2 and SPE statistics and compared them with the corresponding KDE control

limits.

$$\begin{aligned}
 N_g^2 &= \hat{h}_{g,j}^T \hat{h}_{g,j} \leq N_{g,\text{lim}}^2 \\
 SPE_g &= (x_{g,j} - W_g \hat{h}_{g,j})^T (x_{g,j} - W_g \hat{h}_{g,j}) \leq SPE_{g,\text{lim}} \\
 N_i^2 &= \hat{h}_{i,j}^T \hat{h}_{i,j} \leq N_{i,\text{lim}}^2 \\
 SPE_i &= (x_{i,j} - W_i \hat{h}_{i,j})^T (x_{i,j} - W_i \hat{h}_{i,j}) \leq SPE_{i,\text{lim}}
 \end{aligned} \tag{21}$$

where $\hat{h}_{g,j}, \hat{h}_{i,j}, x_{g,j}$ and $x_{i,j}$ are j th column vectors of matrix $\hat{H}_g, \hat{H}_i, X_g$ and X_i respectively. N_g^2, N_i^2, SPE_g and SPE_i denote N^2 and SPE statistics of the global model and i th sub-block model respectively. For each model, the corresponding KDE control limits are $N_{g,\text{lim}}^2, N_{i,\text{lim}}^2, SPE_{g,\text{lim}}$ and $SPE_{i,\text{lim}}$ respectively. If one of $b + 1$ pairs of N^2 and SPE statistics exceeds the corresponding control limit, the fault will be detected.

V. SIMULATION

In this section, the effectiveness of the proposed method is verified by a numerical example and the TE process.

A. A NUMERICAL EXAMPLE

In this paper, a numerical example is used to verify the feasibility of the APNMF method. Consider a simple numerical example proposed by Jiang and Yan [26], as shown below:

$$\begin{bmatrix} x_1 \\ x_2 \\ x_3 \\ x_4 \\ x_5 \\ x_6 \\ x_7 \\ x_8 \\ x_9 \end{bmatrix} = \begin{bmatrix} 0.5768 & 0.3766 & 0 & 0 & 0 & 0 \\ 0.7382 & 0.1566 & 0 & 0 & 0 & 0 \\ 0.8291 & 0.4009 & 0 & 0 & 0 & 0 \\ 0.6519 & 0.2070 & 0 & 0 & 0 & 0 \\ 0 & 0 & 1.7678 & 0.8519 & 0 & 0 \\ 0 & 0 & 1.3936 & 0.8045 & 0 & 0 \\ 0 & 0 & 0.4234 & 0.6654 & 0 & 0 \\ 0 & 0 & 0 & 0 & 0.1000 & 0 \\ 0 & 0 & 0 & 0 & 0 & 0.1000 \end{bmatrix} \times \begin{bmatrix} s_1 \\ s_2 \\ s_3 \\ s_4 \\ s_3 \\ s_3 \\ s_4 \end{bmatrix} + \begin{bmatrix} e_1 \\ e_2 \\ e_3 \\ e_4 \\ e_5 \\ e_6 \\ e_7 \\ e_8 \\ e_9 \end{bmatrix} \tag{22}$$

with $[s_1 \ s_2 \ s_3 \ s_4]^T$ denote the signal sources; $[e_1 \ e_2 \ e_3 \ e_4 \ e_8 \ e_9]^T$ and $[e_5 \ e_6 \ e_7]^T$ are zero-mean Gaussian process noises with standard deviations of 0.01 and 0.08, respectively. The sets of data sources are simulated to generate the following operating modes: s_1 : $U(-10, -9.7)$, s_2 : $N(-5, 1)$, s_3 : $U(3, 4)$, s_4 : $N(3,1)$.

First, 400 samples are generated as training data under normal operating mode. To get the validation data set, the following cases are considered, with each case consisting of 400 samples: 1) a step change of 0.6 is introduced to source s_1 at the 101th point. 2) an ramp change of 0.1($i-100$)

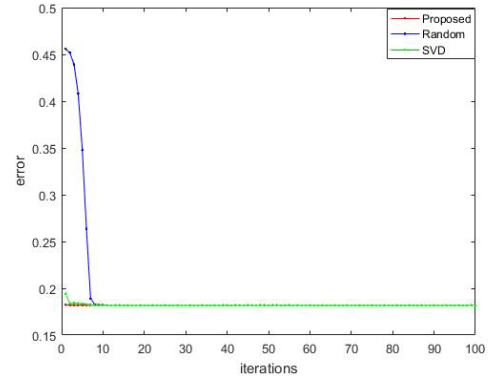


FIGURE 2. The convergence of different initial method.

TABLE 2. Variable partitioning for 2 faults.

| Fault no. | Variable partitioning |
|-----------|--|
| 1 | $C_1(1 \ 2 \ 3 \ 4 \ 8), C_2(5 \ 6 \ 7 \ 9)$ |
| 2 | $C_1(1 \ 2 \ 3 \ 4 \ 8), C_2(5 \ 6 \ 7 \ 9)$ |

is introduced to source s_2 from the 101th point to the 200th point.

In order to show the effectiveness of the proposed initialization method, the paper compares the convergence of different initialization value in Fig.2. The red line is the convergence curve of the proposed method, the blue one is the convergence curve based on SVD, and the green one is the convergence curve based on the random method. As can be seen from Fig.2, the proposed method has faster convergence performance.

With the APNMF method, the results of variable partitioning for each fault are determined by integrating the correlation coefficients and complete linkage algorithm, as shown in Table 2.

The monitoring results of fault 1 based on the global NMF and APNMF methods are shown in Fig. 3. The red line represents the control limit, and the blue line represents the statistical value N^2 or SPE .

Global 9 variables are divided into 2 sub-blocks by APNMF method with $C_1(12348)$ and $C_2(5679)$. The detection results of those 2 sub-blocks are shown in Fig.3 (b)-(c). Both plots show that the variables in the first block contribute more to the fault than those in the second block, which is in accordance with the case that we have designed. As shown in Fig.3, the fault detection rates of N^2 and SPE based on the NMF are 0.1733 and 0.8933 respectively, while those based on the APNMF are 0.2766 and 1 respectively.

The monitoring results of fault 2 are illustrated in Fig. 4. The red line represents the control limit, and the blue line represents the statistical value N^2 or SPE . As shown in Fig. 4(a), the fault detection rate detected by global NMF is not so well, where N^2 statistic is 0.76 and SPE statistic is 0.69. However, the APNMF method can detect the fault with a

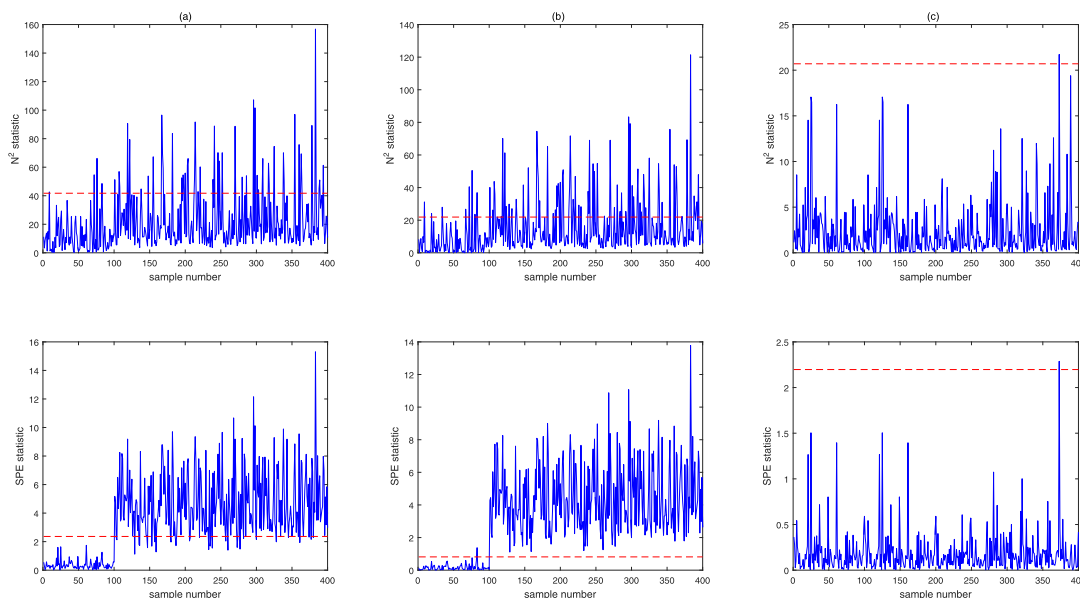


FIGURE 3. Fault detection results for Fault 1. (a) global NMF; (b-c) NMF sub-blocks $C_1 - C_2$.

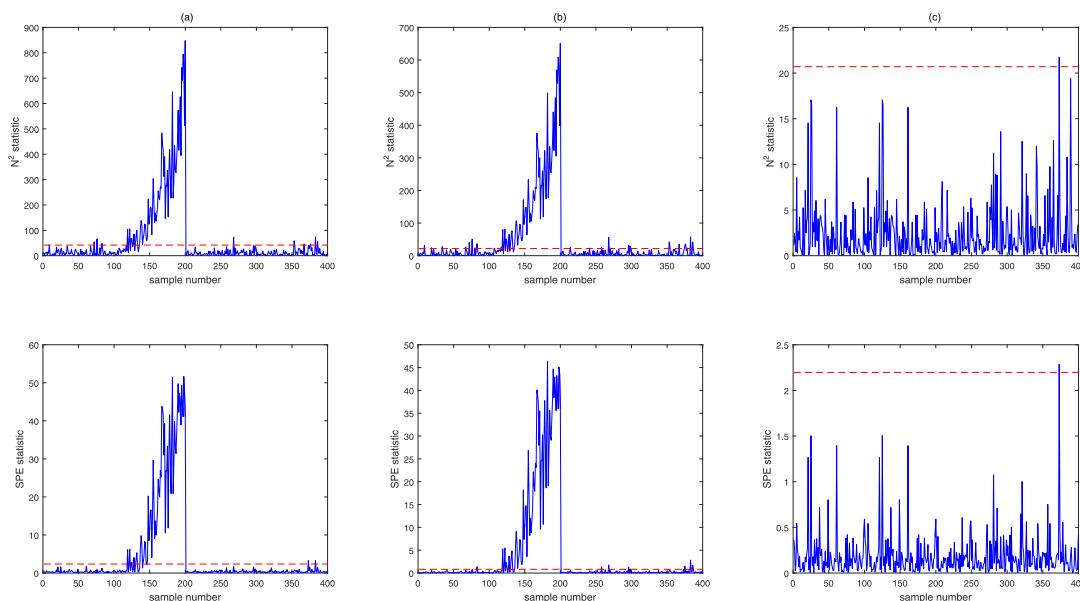


FIGURE 4. Fault detection results for Fault 2. (a) global NMF; (b-c) NMF sub-blocks $C_1 - C_2$.

higher fault detection rate, where N^2 statistic is 0.78 and SPE statistic is 0.75. With the above analysis, the APNMF method is superior to the global NMF and can provide some more correct information for operators.

B. TE BENCHMARK PROCESS

The proposed method is verified by the famous TE chemical process proposed by Downs and Vogel [27] of Eastman Chemical Company, as shown in Fig. 5. The TE process is an effective tool for process fault diagnosis, mainly consisting of five operating units, i.e., reactor, product

condenser, vapor liquid separator, recycle compressor and product stripper. The TE process has 22 continuous measurements, 19 composition measurements and 12 manipulated variables. In this paper, 22 continuous variables and 11 manipulated variables are used for process monitoring, which are listed in Table 3. The plant-wide control structure recommended by Lyman and Georgakis [28] was used to generate simulated process data in this study. The data of TE process can be downloaded from this website: <http://web.mit.edu/braatzgroup/links.html>. 21 faults that are often appeared in TE process are provided in Table 4.

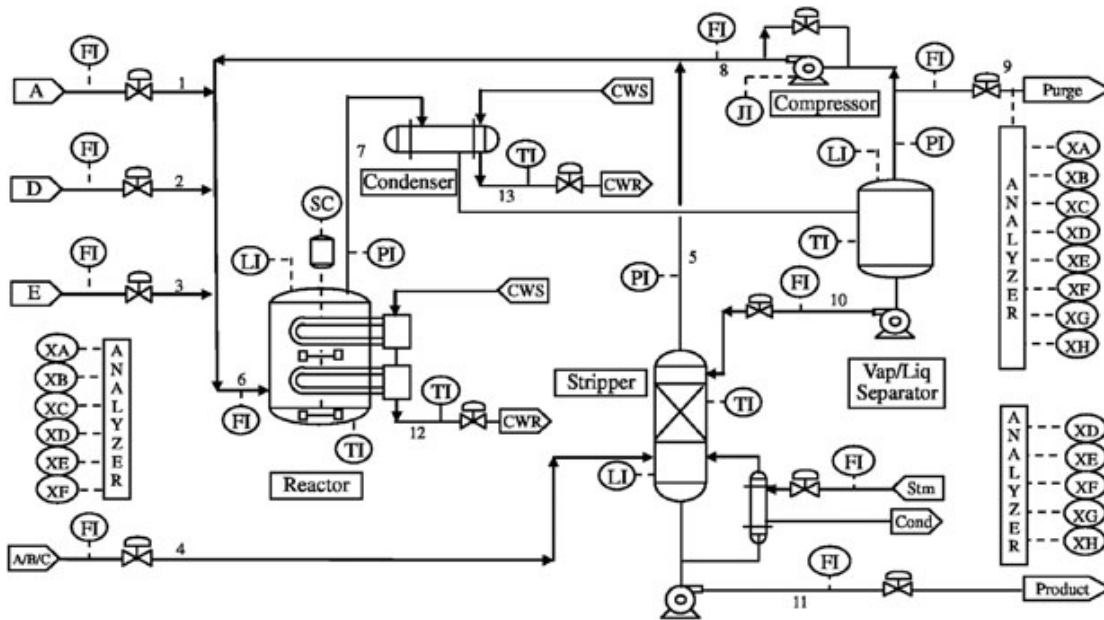


FIGURE 5. Diagram of TE process.

TABLE 3. Selected variables for fault detection in the TE process.

| No. | Description | No. | Description | No. | Description |
|-----|---------------------|-----|----------------------|-----|------------------------------|
| 1 | A Feed | 12 | Product Sep Level | 23 | D Feed Flow |
| 2 | D Feed | 13 | Prod Sep Pressure | 24 | E Feed Flow |
| 3 | E Feed | 14 | Prod Sep Underflow | 25 | A Feed Flow |
| 4 | A and C Feed | 15 | Stripper Level | 26 | A and C Feed Flow |
| 5 | Recycle Flow | 16 | Stripper Pressure | 27 | Compressor Recycle Valve |
| 6 | Reactor Feed Rate | 17 | Stripper Underflow | 28 | Purge Valve |
| 7 | Reactor Pressure | 18 | Stripper Temperature | 29 | Separator Pot Liquid Flow |
| 8 | Reactor Level | 19 | Stripper Steam Flow | 30 | Stripper Liquid Product Flow |
| 9 | Reactor Temperature | 20 | Compressor Work | 31 | Stripper Steam Valve |
| 10 | Purge Rate | 21 | RCW Outlet Temp | 32 | RCW Flow |
| 11 | Product Sep Temp | 22 | SCW Outlet Temp | 33 | CCW Flow |

The normal data with no process fault are used as training data set, which contains 500 samples. 21 test data sets are collected in 21 fault modes and each contains 960 samples. In addition, each fault test data set starts with normal data and the fault is introduced from 161th sample.

To test the APNMF method, the fault detection rate and delay time are chosen as two criterions to assess the monitoring performance, and the monitoring results of the PCA, NMF [11], PNMF [16] and ALS-NMF [19] are given for comparison. If a monitoring technique has a higher detection rate and lower delay time, then this method is determined to have better performance. All the data in TE process need to be preprocessed before the application of

the above algorithms. In the PCA-based monitoring method, the number of principal elements is selected to capture over 85% of data variation. The NMF-based method includes NMF, PNMF, ALS-NMF and APNMF select the same dimension reduction order k as PCA for comparison. The 99% control limits of all the statistic variables are determined by KDE.

With the APNMF method, a series of sub-block models for each fault are built. The results of variable partitioning for each fault are shown in Table 5.

The fault detection results of PCA, NMF, PNMF, ALS-NMF and APNMF are listed in Table 6. The detection results having striking contrast are marked with bold fonts.

TABLE 4. Process faults for the TEP.

| Fault no. | Process variable | Type |
|-----------|--|-------------------|
| Fault 1 | A/C feed ratio, B composition constant (stream 4) | Step |
| Fault 2 | B composition, A/C ratio constant (stream 4) | Step |
| Fault 3 | D feed temperature (stream 2) | Step |
| Fault 4 | Reactor cooling water inlet temperature | Step |
| Fault 5 | Condenser cooling water inlet temperature | Step |
| Fault 6 | A feed loss (stream 1) | Step |
| Fault 7 | C header pressure loss-reduced availability (stream 4) | Step |
| Fault 8 | A, B, C feed composition (stream 4) | Random variation |
| Fault 9 | D feed temperature (stream 2) | Random variation |
| Fault 10 | C feed temperature (stream 2) | Random variation |
| Fault 11 | Reactor cooling water inlet temperature | Random variation |
| Fault 12 | Condenser cooling water inlet temperature | Random variation |
| Fault 13 | Reaction kinetics | Slow drift |
| Fault 14 | Reactor cooling water valve | Sticking |
| Fault 15 | Condenser cooling water valve | Sticking |
| Fault 16 | Unknown | Unknown |
| Fault 17 | Unknown | Unknown |
| Fault 18 | Unknown | Unknown |
| Fault 19 | Unknown | Unknown |
| Fault 20 | Unknown | Unknown |
| Fault 21 | Valve position constant (stream 4) | Constant position |

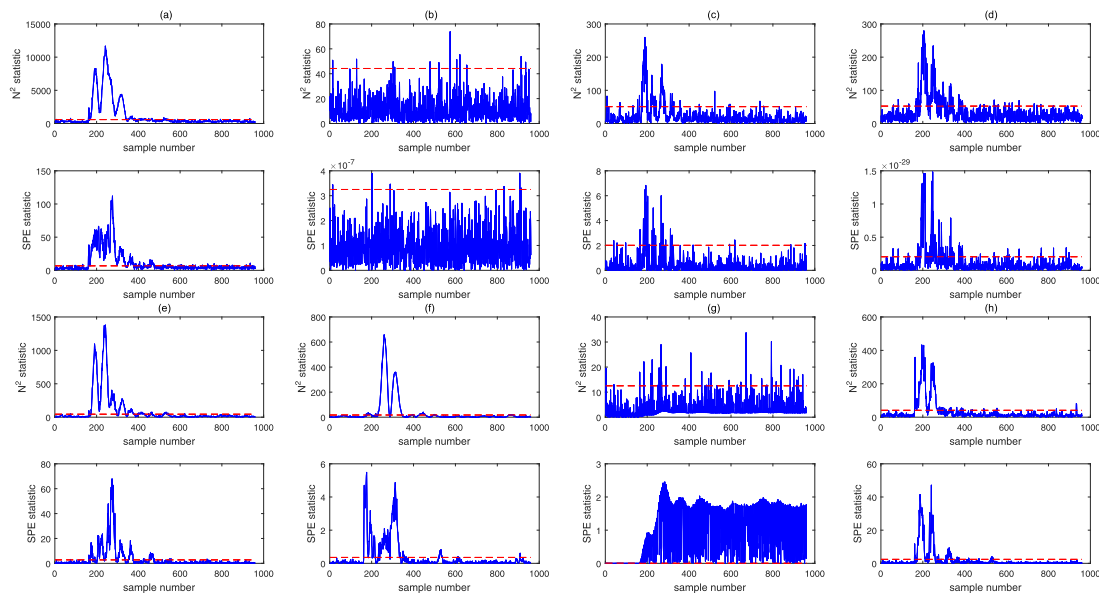


FIGURE 6. Fault detection results for Fault 5. (a) global NMF; (b-h) NMF sub-blocks $C_1 - C_7$.

Noted that the overall effect of the NMF-based method is better than that of the PCA method, which is the same with the published papers [19]–[21]. Compared to PCA, NMF, PNMF, ALS-NMF, the APNMF method shows the highest fault detection rate and minimum delay time in most fault modes, especially in fault modes 3, 5, 9, 10, 16 and 19. It is

easy for the above three methods to detect Fault 1, 2, 6, 7, 8, 12, 13, 14, 17 and 18 because they have an obviously effect on the variation and mean of the overall process. According to the above analysis on the TE process, the proposed APNMF method is demonstrated to perform better in fault monitoring than PCA, NMF, PNMF and ALS-NMF.

TABLE 5. Variable partitioning for 21 faults.

| Fault no. | Variable partitioning |
|-----------|---|
| 1 | {12, 15, 23, 29, 30}; {2, 6, 8, 32}; {1, 4, 7, 11, 16, 20, 25, 27, 33}; {9, 13, 17, 18, 21, 31}; {3, 5}; {14, 19, 24, 26}; {10, 22, 28} |
| 2 | {2, 12, 15, 21, 23, 29, 30}; {7, 13, 18, 19, 20}; {17, 33}; {1, 3, 5, 25}; {4, 14, 24, 26}; {6, 8}; {9, 32}; {10, 16, 27, 28}; {11, 22, 31} |
| 3 | {2, 12, 15, 21, 23, 29, 30}; {6, 8}; {4, 7, 13, 16, 17, 20, 27, 33}; {10, 28}; {14, 24, 26}; {1, 3, 5, 25}; {11, 22}; {9, 32}; {18, 19, 31} |
| 4 | {2, 15, 21, 23, 30}; {1, 3, 5, 25}; {6, 8}; {4, 7, 11, 13, 16, 17, 20, 22, 27, 33}; {18, 19}; {9, 12, 29, 32}; {14, 24, 26, 31}; {10, 28} |
| 5 | {12, 15, 23, 29, 30}; {2, 9, 21, 32}; {3, 5, 6, 8, 14}; {1, 4, 7, 13, 16, 20, 25, 27}; {18, 19, 26, 31}; {17, 33}; {10, 11, 22, 24, 28} |
| 6 | {2, 6, 9, 10, 12, 15, 17, 18, 19, 20, 21, 23, 25, 26, 28, 29, 30, 31, 32, 33}; {1, 3, 4, 7, 11, 13, 22, 27}; {5, 8, 14, 16, 24} |
| 7 | {4, 7, 13, 16, 18, 20, 27, 31, 33}; {2, 3, 14, 19, 32}; {1, 5, 9, 12, 17, 21, 24, 25, 26, 29}; {6, 8, 15, 23, 30}; {10, 11, 22, 28} |
| 8 | {1, 2, 4, 7, 8, 11, 12, 13, 15, 16, 17, 20, 23, 24, 25, 27, 29, 30, 32, 33}; {10, 18, 19, 28}; {26, 31}; {3, 5, 6, 14}; {9, 21, 22} |
| 9 | {2, 12, 15, 21, 23, 29, 30}; {6, 8, 14}; {10, 28}; {24, 26, 31}; {1, 3, 5, 25}; {4, 7, 13, 16, 17, 18, 19, 20, 27, 33}; {9, 32}; {11, 22} |
| 10 | {2, 12, 15, 21, 23, 29, 30}; {10, 28}; {1, 3, 5, 14, 24, 25, 26}; {6, 8}; {9, 32}; {4, 7, 11, 13, 16, 17, 20, 22, 27}; {18, 19, 31, 33} |
| 11 | {15, 23, 30}; {3, 5, 17, 24, 26}; {1, 9, 12, 14, 25, 29, 32}; {6, 8}; {2, 21, 31}; {4, 7, 10, 13, 16, 18, 19, 20, 27, 28, 33}; {11, 22} |
| 12 | {1, 4, 7, 13, 16, 17, 20, 25, 27, 33}; {18, 19, 31}; {3, 5, 6, 14}; {10, 26, 28}; {2, 9, 12, 21, 29, 32}; {8, 15, 23, 30}; {11, 22, 24} |
| 13 | {1, 4, 7, 9, 13, 16, 17, 20, 21, 25, 27, 33}; {2, 11, 12, 15, 24, 29, 30, 32}; {8, 23, 26}; {18, 19}; {3, 5, 10, 22, 28}; {6, 14, 31} |
| 14 | {1, 2, 4, 6, 7, 9, 11, 12, 13, 16, 18, 19, 20, 21, 22, 23, 25, 27, 29, 31}; {3, 5, 24, 26}; {14, 32}; {8, 15, 17, 30, 33}; {10, 28} |
| 15 | {12, 15, 23, 29, 30}; {2, 21}; {6, 14}; {9, 32}; {10, 28}; {1, 3, 5, 24, 25, 26}; {4, 7, 11, 13, 16, 17, 20, 22, 27}; {8, 33}; {18, 19, 31} |
| 16 | {2, 12, 15, 21, 23, 29, 30}; {6, 8, 14}; {9, 32}; {10, 28}; {18, 19, 31}; {1, 3, 5, 24, 25, 26}; {4, 7, 11, 13, 16, 17, 20, 22, 27, 33} |
| 17 | {2, 3, 4, 5, 6, 7, 8, 10, 12, 13, 14, 15, 16, 17, 18, 21, 22, 23, 24, 26, 27, 29, 30, 31, 33}; {1, 9, 11, 19, 20, 25, 28, 32} |
| 18 | {1, 2, 3, 5, 6, 7, 8, 9, 10, 12, 13, 15, 16, 17, 18, 19, 20, 21, 23, 25, 26, 28, 29, 30, 32, 33}; {4, 27, 31}; {8, 11, 22, 24} |
| 19 | {2, 12, 15, 21, 23, 29, 30}; {9, 32}; {3, 5, 25}; {16, 17, 20, 33}; {10, 28}; {18, 19, 31}; {1, 24, 26}; {6, 8, 14}; {4, 7, 11, 13, 22, 27} |
| 20 | {2, 15, 17, 22, 30, 32}; {3, 5, 24, 26}; {1, 4, 7, 9, 11, 16, 20, 21, 25, 27, 33}; {6, 8, 14}; {10, 28}; {13, 18, 19, 31}; {12, 23, 29} |
| 21 | {4, 6, 7, 8, 10, 11, 13, 14, 16, 18, 19, 20, 27, 28, 31}; {9, 32}; {1, 22}; {3, 5, 24, 25}; {2, 12, 15, 21, 23, 29, 30}; {17, 33}; {26} |

Specifically, let's take Fault 5 as an example. Fault 5 is a step change in the condenser cooling water inlet temperature. The detection results based on the global NMF and APNMF methods are shown in Fig. 6. The red line represents the control limit, and the blue line represents the statistical value N^2 or SPE . As shown in Fig. 6(a), the fault is clearly detected between the 161th sample and 385th sample by the global NMF. However, the fault is hard to detect after 385th sample owing to the compensation of the control loop. Global 33 variables are divided into 7 sub-blocks by the APNMF method with $C_1(12, 15, 23, 29, 30)$, $C_2(2, 9, 21, 32)$, $C_3(3, 5, 6, 8, 14)$, $C_4(1, 4, 7, 13, 16, 20, 25, 27)$, $C_5(18, 19, 26, 31)$, $C_6(17, 33)$ and $C_7(10, 11, 22, 24, 28)$. The detection results of those 7 sub-blocks are shown in Fig. 6(b)-(h). The same low detection results as shown in Fig. 6(a) exist in the six sub-blocks (b, c, d, e, f, h). However, sub-block C_6 can detect the fault by the SPE statistic almost in the whole fault operation,

as shown in Fig. 6(g). The fault detection rates of N^2 and SPE based on the NMF are 0.3300 and 0.3612 respectively, while those based on the APNMF are 0.4762 and 0.9924 respectively. The SPE statistic of APNMF will continue to inform the operators that the fault still remains in the process and sub-block C_6 takes the most responsibility for fault detection.

Fault 10 is a random change in the C feed temperature. The detection results based on the global NMF and APNMF methods are shown in Fig. 7. The red line represents the control limit, and the blue line represents the statistical value N^2 or SPE . As shown in Fig. 7(a), the fault detection rate detected by global NMF is low, where N^2 statistic is 0.5538 and SPE statistic is 0.5737, and nearly half of the failure samples have not been detected. However, the APNMF method can detect the fault with a higher fault detection rate, where N^2 statistic SPE is 0.7063 and statistic is 0.8562. Global 33 variables are

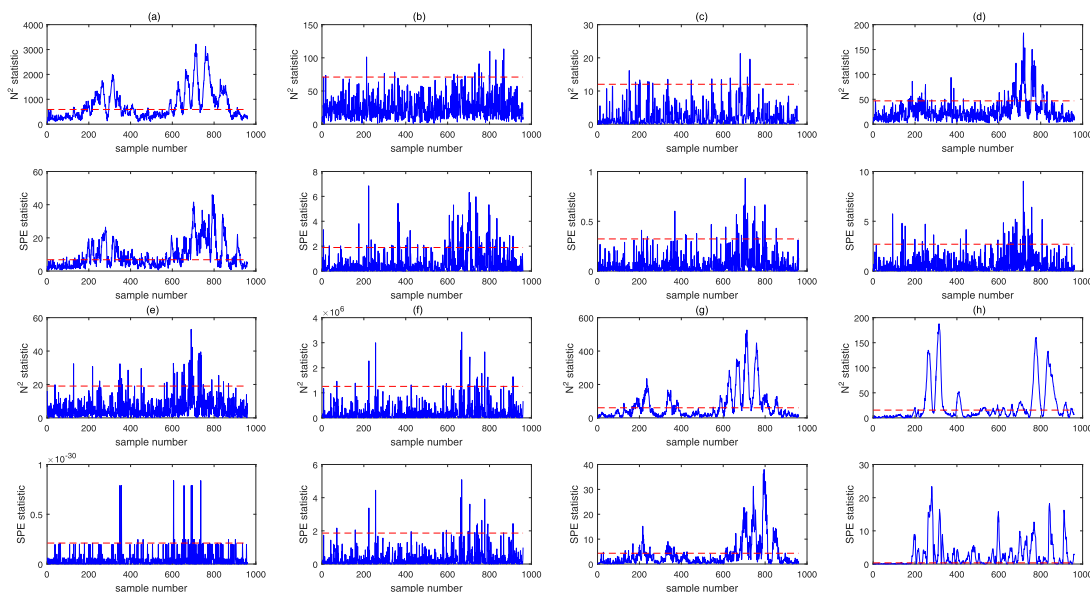


FIGURE 7. Fault detection results for Fault 10. (a) global NMF; (b-h) NMF sub-blocks $C_1 - C_7$.

TABLE 6. Fault detection results /delayed time in 21 fault modes.

| Fault No. | Fault detection rates (%)/delay time | | | | | | | | | |
|-----------|--------------------------------------|----------------|----------------|---------------|----------------|---------------|----------------|----------------|----------------|----------------|
| | PCA | | NMF | | PGNMF | | ALS-NMF | | APNMF | |
| | T ² | SPE | N ² | SPE | N ² | SPE | N ² | SPE | N ² | SPE |
| 1 | 99.3/6 | 100/0 | 99.6/3 | 97.4/3 | 99.3/6 | 96.6/3 | 99.5/4 | 99.4/0 | 99.9/0 | 99.1/0 |
| 2 | 98.3/14 | 99/7 | 98.4/12 | 96.8/9 | 98.3/14 | 96.9/16 | 98.5/12 | 97.4/4 | 98.9/5 | 98.3/4 |
| 3 | 6.3/14 | 4.9/51 | 10.4/14 | 8.8/17 | 4.6/14 | 9.3/17 | 6.1/14 | 10.9/17 | 38.5/4 | 24.5/18 |
| 4 | 31.1/0 | 100/0 | 77.5/0 | 99.2/0 | 96.5/0 | 99.3/0 | 86.4/0 | 99.5/0 | 99/0 | 100/0 |
| 5 | 27.8/0 | 26.9/0 | 33/0 | 36.1/0 | 27/0 | 36.8/0 | 29/0 | 38.1/0 | 47.6/0 | 99.2/0 |
| 6 | 99.4/4 | 100/0 | 100/0 | 99.9/1 | 100/0 | 99.9/1 | 100/0 | 99.9/1 | 100/0 | 100/0 |
| 7 | 100/0 | 100/0 | 97.8/0 | 100/0 | 88.3/0 | 100/0 | 99.1/0 | 100/0 | 100/0 | 100/0 |
| 8 | 97.4/14 | 94.9/8 | 98/9 | 97.3/7 | 98.1/9 | 97.3/7 | 98/9 | 97.6/7 | 98.4/8 | 98.9/7 |
| 9 | 5.3/0 | 4.6/3 | 7.8/0 | 16.5/0 | 4.4/2 | 17.1/0 | 5.9/2 | 16.6/0 | 25.3/0 | 31.1/0 |
| 10 | 45.6/5 | 49.6/26 | 55.4/7 | 57.4/5 | 49.9/15 | 57.9/5 | 51.5/15 | 58.9/5 | 70.6/4 | 85.6/5 |
| 11 | 48.1/5 | 80.5/25 | 69/5 | 68.3/5 | 73.3/5 | 68.6/5 | 69.5/5 | 72/5 | 75.3/5 | 80.8/5 |
| 12 | 98.5/2 | 94.6/2 | 99.4/2 | 98.3/2 | 99/2 | 98.3/2 | 99.3/2 | 98.6/2 | 99.5/2 | 99.3/2 |
| 13 | 94.3/46 | 95.3/37 | 94.8/41 | 93.8/20 | 94.3/46 | 93.8/20 | 94.6/46 | 93.8/20 | 95.3/14 | 96/13 |
| 14 | 99.5/0 | 100/0 | 100/0 | 99.9/1 | 100/0 | 99.9/1 | 100/0 | 99.9/1 | 100/0 | 100/0 |
| 15 | 8.5/77 | 8.3/16 | 19/91 | 10.8/16 | 11.8/94 | 11.1/16 | 14.4/94 | 12.4/16 | 32.1/18 | 23.8/16 |
| 16 | 30/33 | 47.6/15 | 43.9/30 | 55.8/0 | 34.9/30 | 55.9/0 | 38.4/30 | 57.6/0 | 67/18 | 90.4/0 |
| 17 | 80/1 | 96/19 | 89.3/23 | 95.3/20 | 89/23 | 95.4/20 | 88.8/23 | 95.6/20 | 90.6/1 | 96.3/0 |
| 18 | 89.9/18 | 90.5/15 | 90.5/56 | 91.4/3 | 89.9/60 | 91.4/3 | 90.3/60 | 91.4/3 | 91.5/17 | 92.1/3 |
| 19 | 14.5/10 | 28.8/11 | 10.3/10 | 37.3/1 | 7.6/10 | 36.8/1 | 15.3/10 | 34.3/1 | 37.9/2 | 59.1/1 |
| 20 | 42.5/74 | 60/62 | 55.5/5 | 67/4 | 49/5 | 67.3/4 | 52.5/5 | 68.5/4 | 71.9/5 | 79/1 |
| 21 | 40.6/33 | 56.1/1 | 46/250 | 47.5/0 | 41.4/250 | 47.9/0 | 43.3/250 | 50/0 | 53.5/0 | 65.5/0 |

divided into 7 sub-blocks with C_1 (15, 30, 23, 12, 29, 2, 21), C_2 (10, 28), C_3 (1, 25, 3, 5, 14, 24, 26), C_4 (6, 8), C_5 (9, 32), C_6 (4, 27, 16, 7, 13, 20, 17, 11, 22) and C_7 (18, 19, 31, 33). Fig. 7 (h) shows that the sub-block C_7 model has a high

sensitivity to Fault 10 where the fault detection rate for N^2 and SPE statistics are 0.4325 and 0.7712 respectively. On the other hand, the other 6 sub-block models have a lower sensitivity to Fault 10. With the above analysis,

the APNMF method is superior to the global NMF and can provide some more correct information for operators.

VI. CONCLUSION

In this work, a new method has been developed to enhance fault monitoring for non-Gaussian processes based on APNMF method. The proposed fault monitoring method mainly includes three stages, which are global fault monitoring, data adaptive partitioning and block fault monitoring. In global fault monitoring, the residuals of online operating data are collected by performing NMF upon the whole variables. Then, the variables are partitioned into several blocks by integrating the residuals and complete linkage algorithm. Finally, a series of sub-block NMF models are constructed and used to realize block fault monitoring. The sub-block NMF model is dynamically updated under different operation conditions, which broadens the applicability of this method. Besides, the method improves monitoring performance by making full use of global information between the block and local information within the block. The study of a numerical example and the TE process show that this method can improve the accuracy in fault monitoring. However, this paper only discusses fault monitoring in non-Gaussian processes without considering the nonlinearity of industrial processes. The fault diagnosis in nonlinear processes will be the future research direction.

REFERENCES

- [1] M. Kano and Y. Nakagawa, "Data-based process monitoring, process control, and quality improvement: Recent developments and applications in steel industry," *Comput. Chem. Eng.*, vol. 32, nos. 1–2, pp. 12–24, 2008.
- [2] J. Yu, "Fault detection using principal components-based Gaussian mixture model for semiconductor manufacturing processes," *IEEE Trans. Semicond. Manuf.*, vol. 24, no. 3, pp. 432–444, Aug. 2011.
- [3] G. Li, S. J. Qin, and D. Zhou, "Geometric properties of partial least squares for process monitoring," *Automatica*, vol. 46, no. 1, pp. 204–210, 2010.
- [4] P.-E. P. Odiwei and Y. Cao, "Nonlinear dynamic process monitoring using canonical variate analysis and kernel density estimations," *IEEE Trans. Ind. Informat.*, vol. 6, no. 1, pp. 36–45, Feb. 2010.
- [5] Y. Zhang and S. J. Qin, "Fault detection of nonlinear processes using multiway kernel independent component analysis," *Ind. Eng. Chem. Res.*, vol. 46, no. 23, pp. 7780–7787, 2007.
- [6] E. Cai, D. Liu, L. Liang, and G. Xu, "Monitoring of chemical industrial processes using integrated complex network theory with PCA," *Chemometrics Intell. Lab. Syst.*, vol. 140, pp. 22–35, Jan. 2015.
- [7] D. S. Lee and P. A. Vanrolleghem, "Monitoring of a sequencing batch reactor using adaptive multiblock principal component analysis," *Biotechnol. Bioeng.*, vol. 82, no. 4, pp. 489–497, 2003.
- [8] K. Liu, X. Jin, Z. Fei, and J. Liang, "Adaptive partitioning PCA model for improving fault detection and isolation," *Chin. J. Chem. Eng.*, vol. 23, no. 6, pp. 981–991, Jun. 2015.
- [9] Z. Ge and Z. Song, "Process monitoring based on independent component analysis-principal component analysis (ICA-PCA) and similarity factors," *Ind. Eng. Chem. Res.*, vol. 46, no. 7, pp. 2054–2063, 2007.
- [10] G. Stefatos and A. B. Hamza, "Dynamic independent component analysis approach for fault detection and diagnosis," *Expert Syst. Appl.*, vol. 37, no. 12, pp. 8606–8617, 2010.
- [11] X. Long, H. Lu, Y. Peng, and W. Li, "Graph regularized discriminative non-negative matrix factorization for face recognition," *Multimedia Tools Appl.*, vol. 72, no. 3, pp. 2679–2699, 2014.
- [12] B. Du, Z. Wang, L. Zhang, L. Zhang, and D. Tao, "Robust and discriminative labeling for multi-label active learning based on maximum correntropy criterion," *IEEE Trans. Image Process.*, vol. 26, no. 4, pp. 1694–1707, Apr. 2017.
- [13] B. Du, T. Xinyao, Z. Wang, L. Zhang, and D. Tao, "Robust graph-based semisupervised learning for noisy labeled data via maximum correntropy criterion," *IEEE Trans. Cybern.*, vol. 49, no. 4, pp. 1440–1453, Apr. 2019.
- [14] D. D. Lee and H. S. Seung, "Learning the parts of objects by non-negative matrix factorization," *Nature*, vol. 401, pp. 788–791, Oct. 1999.
- [15] D. D. Lee and H. S. Seung, "Algorithms for non-negative matrix factorization," in *Proc. Adv. Neural Inf. Process. Syst.*, 2001, pp. 556–562.
- [16] C.-J. Lin, "Projected gradient methods for nonnegative matrix factorization," *Neural Comput.*, vol. 19, no. 10, pp. 2756–2779, 2007.
- [17] A. K. Ch, "Mining association rules using non-negative matrix factorization and formal concept analysis," in *Proc. Int. Conf. Inf. Process.*, Aug. 2011, pp. 31–39.
- [18] K. Allab, L. Labiod, and M. Nadif, "Simultaneous semi-NMF and PCA for clustering," in *Proc. IEEE Int. Conf. Data Mining*, Nov. 2016, pp. 679–684.
- [19] X.-B. Li, Y.-P. Yang, and W.-D. Zhang, "Fault detection method for non-Gaussian processes based on non-negative matrix factorization," *Asia-Pacific J. Chem. Eng.*, vol. 8, no. 3, pp. 362–370, 2013.
- [20] X. Li, Y. Yang, and W. Zhang, "Statistical process monitoring via generalized non-negative matrix projection," *Chemometrics Intell. Lab. Syst.*, vol. 121, no. 7, pp. 15–25, 2013.
- [21] Y. Chen, M. Li, L. Liang, G. Xu, and H. Gao, "Feature extraction for fault diagnosis utilizing supervised nonnegative matrix factorization combined statistical model," in *Proc. 9th Int. Congr. Image Signal Process., BioMed. Eng. Inf.*, Datong, China, Oct. 2017, pp. 1188–1193.
- [22] H. Zhu, F. Wang, H. Shi, and S. Tan, "Fault detection method for chemical process based on LPP-GNMF algorithm," *Chin. Autom. Congr.*, vol. 67, no. 12, pp. 5155–5162, 2016.
- [23] N. Li and Y. Yang, "Using semi-nonnegative matrix underapproximation for statistical process monitoring," *Chemometrics Intell. Lab. Syst.*, vol. 153, pp. 126–139, Apr. 2016.
- [24] A. R. Mugdadi and I. A. Ahmad, "A bandwidth selection for kernel density estimation of functions of random variables," *Comput. Stat. Data Anal.*, vol. 47, no. 1, pp. 49–62, 2004.
- [25] E. V. Djukova and N. V. Pekov, "A classification algorithm based on the complete decision tree," *Pattern Recognit. Image Anal.*, vol. 17, no. 3, pp. 363–367, 2007.
- [26] Q. Jiang and X. Yan, "Monitoring multi-mode plant-wide processes by using mutual information-based multi-block PCA, joint probability, and Bayesian inference," *Chemometrics Intell. Lab. Syst.*, vol. 136, no. 9, pp. 124–137, 2014.
- [27] J. J. Downs and E. F. Vogel, "A plant-wide industrial process control problem," *Comput. Chem. Eng.*, vol. 17, no. 3, pp. 245–255, 1993.
- [28] P. R. Lyman and C. Georgakis, "Plant-wide control of the Tennessee eastman problem," *Comput. Chem. Eng.*, vol. 19, no. 3, pp. 321–331, 1995.



YAN WANG was born in Henan, China, in 1986. She received the B.S. degree in automation from Henan University, Kaifeng, China, in 2008, the M.S. degree in control science and engineering from the Wuhan University of Technology, Wuhan, China, in 2011, and the Ph.D. degree in control science and engineering from the Huazhong University of Science and Technology, Wuhan, in 2015. Since 2015, she has been a Lecturer with the School of Electrical and Information Engineering, Zhengzhou University of Light Industry, Zhengzhou, China. Her research interests include systems' identification, fault diagnosis, and controller performance analysis.



SHI-MENG YUAN was born in Henan, China, in 1993. He received the bachelor's degree in automation from the Zhengzhou University of Light Industry, in 2017, where he is currently pursuing the master's degree in control theory and engineering. His research interests include systems' identification and fault diagnosis.



DAN LING was born in Henan, China, in 1986. She received the B.S. degree in automation from the Kunming University of Science and Technology, Kunming, China, in 2010, and the Ph.D. degree in control science and engineering from the Huazhong University of Science and Technology, Wuhan, China, in 2018. Since 2018, she has been a Lecturer with the School of Electrical and Information Engineering, Zhengzhou University of Light Industry. Her research interests include fault diagnosis, model plant mismatch diagnosis, control performance assessment, and statistical process control.



XIAO-GUANG GU was born in Henan, China, in 1986. He received the B.S. degree in automation and the M.S. degree in applied mathematics from Henan University, Kaifeng, China, in 2008 and 2011, respectively, and the Ph.D. degree in control science and engineering from the Nanjing University of Science and Technology, Nanjing, China, in 2018. Since 2018, he has been a Faculty Member with the School of Business, Nanjing University. His research interests include parameter design, tolerance design, process capability analysis, six sigma management, and value chain management.



YU-BO ZHAO was born in Henan, China, in 1996. She is currently pursuing the bachelor's degree in automation with the Zhengzhou University of Light Industry. Her main research interests include fault diagnosis and controller performance analysis.



BO-YI LI was born in Henan, China, in 1996. He is currently pursuing the bachelor's degree in automation with the Zhengzhou University of Light Industry. His main research interests include fault diagnosis and controller performance analysis.

...